Trigger and selection studies for the decay $D^0 \to h^+h^-\pi^0$

Salvatore Tesoro
Supervisor: Dr Mika Anton Vesterinen

August 10, 2012

Abstract

Charm physics is proving to be one of the most exciting areas of research in probing physics beyond the Standard Model. High precision measurements of CP violation can shine light on the matter-antimatter asymmetry in our universe. The study of $D^0 \to h^+h^-\pi^0$ ($h = K, \pi$) is very important to this end.

1.1 Introduction

The full analysis on the 2011 LHCb data has recently observed CP violation in D^0 decays differing to 3.9σ from Standard Model predictions. In order to further increase the precision on the CP violation measurements, it is necessary to study as many decay modes of the D^0 meson as precisely as possible[1]. Consider the following decays: $D^{*+} \to D^0\pi^+$ and $D^{*-} \to \overline{D^0}\pi^-$. The slow pion charge determines the flavour of the charm meson involved in the weak decay. The D^{*+} can then continue the chain decaying into a π^0, a K^- and a π^+ or into a π^0 and 2 pions or two kaons of opposite charge. Such modes are very challenging to reconstruct in the LHCb detector, since the π^0 cannot be reconstructed in the HLT, backgrounds are relatively large, it is not possible to vertex the π^0 with the D^0 and the π^0 energy resolution is relatively poor[2][3]. The first part of the project consists in analysing data from the 2011 LHCb measurements and comparing it with Monte Carlo simulated data sets. This project focuses on the 2 pions decays and kaon pion decays of the D^{*+} meson. Firstly, the kinematic variables of the triggered selected data are plotted. Subsequently, selection cuts are chosen and applied to the data with the aim to optimise the signal to background ratio. The kinematic variables of such selected data samples are also plotted and compared with trigger selected data plots. Afterwards, in order to study the efficiency of the cuts applied, Dalitz plots with and without selection cuts applied are created, as it will be described further on. In the final part of the project, trigger efficiencies are studied, for which the analysis of the previous plots is useful in suggesting trigger configurations. [1]

2 Offline selection studies

2.1 Data selection

Here the $D^0 \to \pi^+ K^- \pi^0$ decay is analysed. The D^0 mass distributions before and after the selection cuts are shown in Fig 1. The applied cuts are:

- Kaon delta-log-likelihood > 10
- Pion delta-log-likelihood < -2
- Kaon $p_T > 800$ MeV
- Pion $p_T > 800$ MeV
- π^0 $p_T > 1500$ MeV
- D vertex is downstream of B vertex
- $3100 < m(B) < 4800$ MeV
- Bplus $p_T > 6$ MeV
- Write B^+ impact parameter < 0.3 mm
- D $p_T > 4$ MeV
- D Impact parameter< 0.5 mm
- D OWNPV Chi squared < 50
- $125 < m(\pi^0) < 146$ MeV
- π^0 $\cos\theta > -0.7$.

Applying these cuts selects 45033 events out of 630671. The RMS for the mass distribution of the D^0 is reduced from 79.81 to 55.44, indicating a successful background reduction.

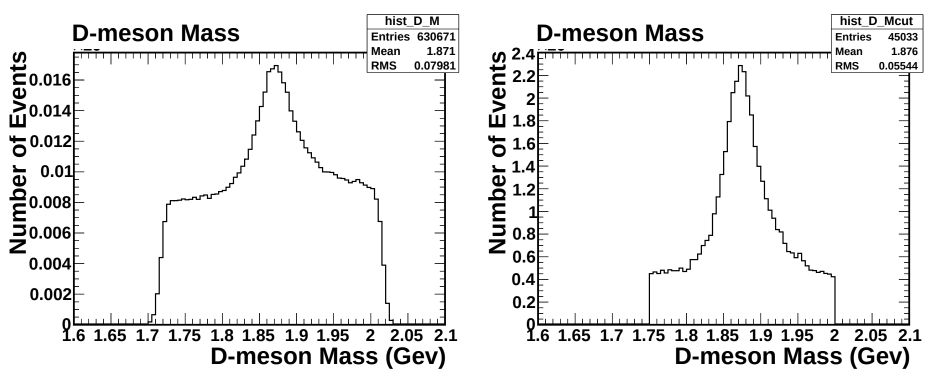

Figure 1: D^0 mass distribution before and after selection cuts

[1] Charge conjugate states are implied throughout this document

2.2 Decay analysis

From the decay products, namely the kaon, pion and π^0, the dynamical properties of the D^0 are reconstructed and plotted before and after the cuts. It is interesting to observe that the geometry of the detector has to be taken into account when analysing the plotted decay variables. For instance, the azimuthal angle does not present an isoptropic distribution for any of the products, because of the quadrangolar nature of the detector. Furthermore, particles travelling precisely parallel to the z-axis of the beam go undetected because the detector is uncovered at its centre (i.e. for $x, y = 0$ trajectories). Particles with high enough transverse momentum do not reach the detector and slow particles are critically deflected. The following plots are examples of such features: Fig. 2a should have less sharp distribution tails (particles were not detected because of too high transverse momentum) and Fig. 2b should display an isotropic distribution.

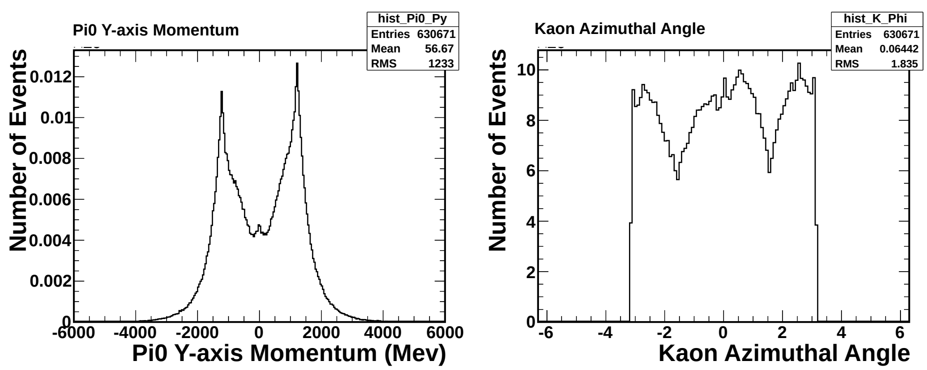

Figure 2: π^0 Y-axis momentum and kaon azimuthal angle

2.3 Decay kinematics

Dalitz plots are some of the most powerful tools in highlighting resonances in three body decays. This feature can be important in illustrating CP violation phenomena. Consider two mirror decays of a particle and its antiparticle, perfectly symmetric decays should display resonances at exactly the same locations and magnitudes. CP violation implies differences in such plots and if the magnitude of such differences is larger than predicted from the Standard Model, they can be hints of new physics. In Fig 3, one of the Dalitz plots representing the decay is presented. The plot shown is obtained after the cuts in section 2.1 have been applied.

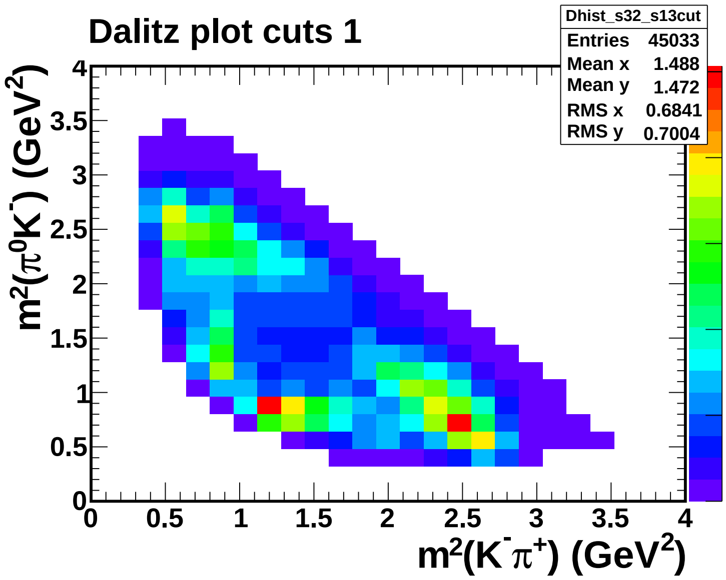

Figure 3: Dalitz plot $D^0 \to K^-\pi^+\pi^0$

2.4 Background subtracted section efficiency across the Dalitz plots

Fig 5 shows one of the background subtracted efficiency plots. They are obtained by subtracting the background events from the histograms before calculating the efficiency. This is done employing the assumption of a flat background. This assumption is justified by the gaussian and polynomial fits shown in Fig 4. Selection efficiency across the Dalitz plots diagrams are obtained dividing the number of entries before applying the cuts by the number of entries after the selection cuts have been applied, for each point in the plots.

3 HLT efficiency studies

3.1 The Hlt2CharmHadD02hhXDst line

Some of the applied cuts are (in units of MeV):

- $\pi_{\rm soft} p_T > 300$
- ($\pi_{\rm soft}+ \pi^+ + \pi^-$) $p_T > 3750$
- ($\pi^+ +\pi^-$)_M<= 1900
- ($\pi_{\rm soft}+ \pi^+ + \pi^-$)_ M $-$ ($\pi^+ + \pi^-$)_M) <= 250
- ($\pi^- p_T >= 1700$ MeV) or (π^+ $p_T > 1700$)

Applying these cuts selects 49680 events out of 932823.

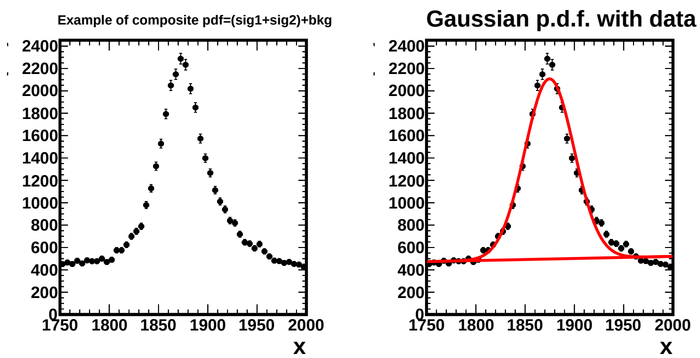

Figure 4: Polynomial and gaussian D^0 mass fits

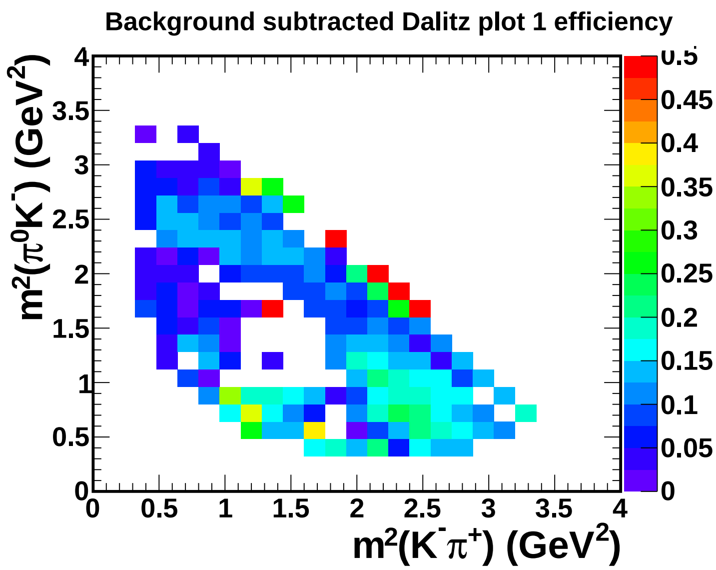

Figure 5: Dalitz plot 1 background subtracted efficiency

3.2 Monte Carlo simulation of $D^0 \to \pi^+ K^- \pi^0$

The decay sequence analysed is $D^{*+} \to D^0 \to \pi^+ K^- \pi^0$. The data come from a Monte Carlo simulation of the decay.

3.2.1 Plots of cut variables

Fig 6 shows plots of the variables the cuts have been applied on. For each variable plotted all cuts but the one on the variable itself have been implemented. The red line indicates that the cut has been placed for values smaller than the line x-coordinate and the blue lines indicate that the cut is for values greater than the line x-coordinate. The last plot shows the maximum between the kaon and pion transverse momentum.

3.2.2 Dalitz plots

Fig 7 displays the Dalitz plots before and after the cuts applied, while Fig 8 shows the efficiency across the Dalitz plot for the selected $m^2(K^-\pi^+)$ versus $m^2(\pi^0 K^-)$ variables. Fig 9 shows the projection of the plot in Fig 8 on the X-axis and on the Y-axis.

3.3 Monte Carlo simulation of $D^0 \to \pi^+\pi^-\pi^0$

The dacay sequence analysed is $B^+ \to D^{*+} \to D^0\pi^+ \to \pi^+\pi^-\pi^0$. The data come from a Monte Carlo simulation of the decay.

3.3.1 Plots of cut variables

Fig 10 displays plots of the variables the cuts have been applied on the $D^0 \to \pi^+\pi^-\pi^0$ MC . The last plot shows the maximum between the 2 charged pions transverse momentum.

3.3.2 Dalitz plots

Fig 11 shows the Dalitz plots before and after applying the cuts, while Fig 12 shows the efficiency across the Dalitz plot for the selected $m^2(\pi^-\pi^+)$ versus $m^2(\pi^0\pi^-)$ variables.

3.4 Optimisation of the cuts

The Default trigger settings for the HLT2 line are:

- SlowPion PT : 300.0 ∗ MeV
- SlowPion PT : 3000.0 ∗ MeV
- Chi2_SlowPion : 2.25
- Chi2_MAX_Child_MAX : 2.25
- IPCHI2_MAX_Child_MIN : 36.
- IPCHI2_PiSlow_MAX : 9.
- PairMaxDoca_Dstar : 10.0 ∗ mm
- PT_Dstar_MIN : 3750.0 ∗ MeV
- DIRA_D0_MIN : 0.999
- FDCHI2_D0_MIN : 100.
- VCHI2_D0_MAX : 10.
- M_MAX : 1900.
- DeltaM_MIN : 0.0 ∗ MeV
- DeltaM_MAX : 250.0 ∗ MeV
- DeltaM_MINwide : 0.0 ∗ MeV
- DeltaM_MAXwide : 500.0 ∗ MeV

Looking at the selection cuts in Fig 6, it is possible to observe which cuts were too extreme and which ones too relaxed. Studying these plots can allow us to improve the efficiency of our trigger.
Keeping this in mind, the project moves on to simulating HLT2 trigger efficiencies for the selected $D^0 \to \pi^+ K^- \pi^0$ decay mode. The two variables of interest in this study are the MonteCarlo efficiency: the number of decay that would be reconstructed in our detector if this were the only decay mode taking place; and the non biased efficiency: the number of decays of all type that would be reconstructed with the proposed HLT2 selection. The first one tells us how many interesting events we are able to reconstruct, while the second is a measure of the size of all raw data that we would collect with this HLT2 trigger level.
A simulation with 190 MC events and 20000 non biased events with is carried out. The default trigger had an MC efficiency of 14.2 ± 2.5 and a non biased efficiency of 0.975 ± 0.067. Efficiencies of other selections are shown in Fig 13.

4 Conclusion

MC simulations efficiencies vary in the range from 14.2 ± 2.5 to 15.3 ± 2.6 for the considered trigger selections. Efficiencies for the trigger simulations on the non biased sample oscillate between 0.975 ± 0.070 and 1.212 ± 0.077.
The statistical uncertainties do not allow us to compare the MC efficiencies of the various trigger combinations. This is due to the size of the MC sample, which should be increased for a precise trigger study. However, a number of trigger combinations have no bias efficiencies lower than the default no bias efficiency and could be used as a starting point for future trigger combinations studies.

References

[1] "The LHCb collaboration", "LHCbDeltaACP", available at "https://lhcb-reconstruction.web.cern.ch/lhcb-reconstruction/2012/deltaACP/", August 1st 2012.

[2] "The LHCb collaboration","Evidence for CP violation in time-integrated D0 hh+ decay rates", page 3-4, Phys. Rev. Lett. 108 (2012) 111602, March 19th 2012.

[3] "The BABAR Collaboration, B. Aubert, et al", "Precise Branching Ratio Measurements of the Decays $D0 \to pi - pi + pi0$ and $D0 \to K - K + pi0$", page 4-5, Phys.Rev.D74:091102,2006 August 3rd 2006.

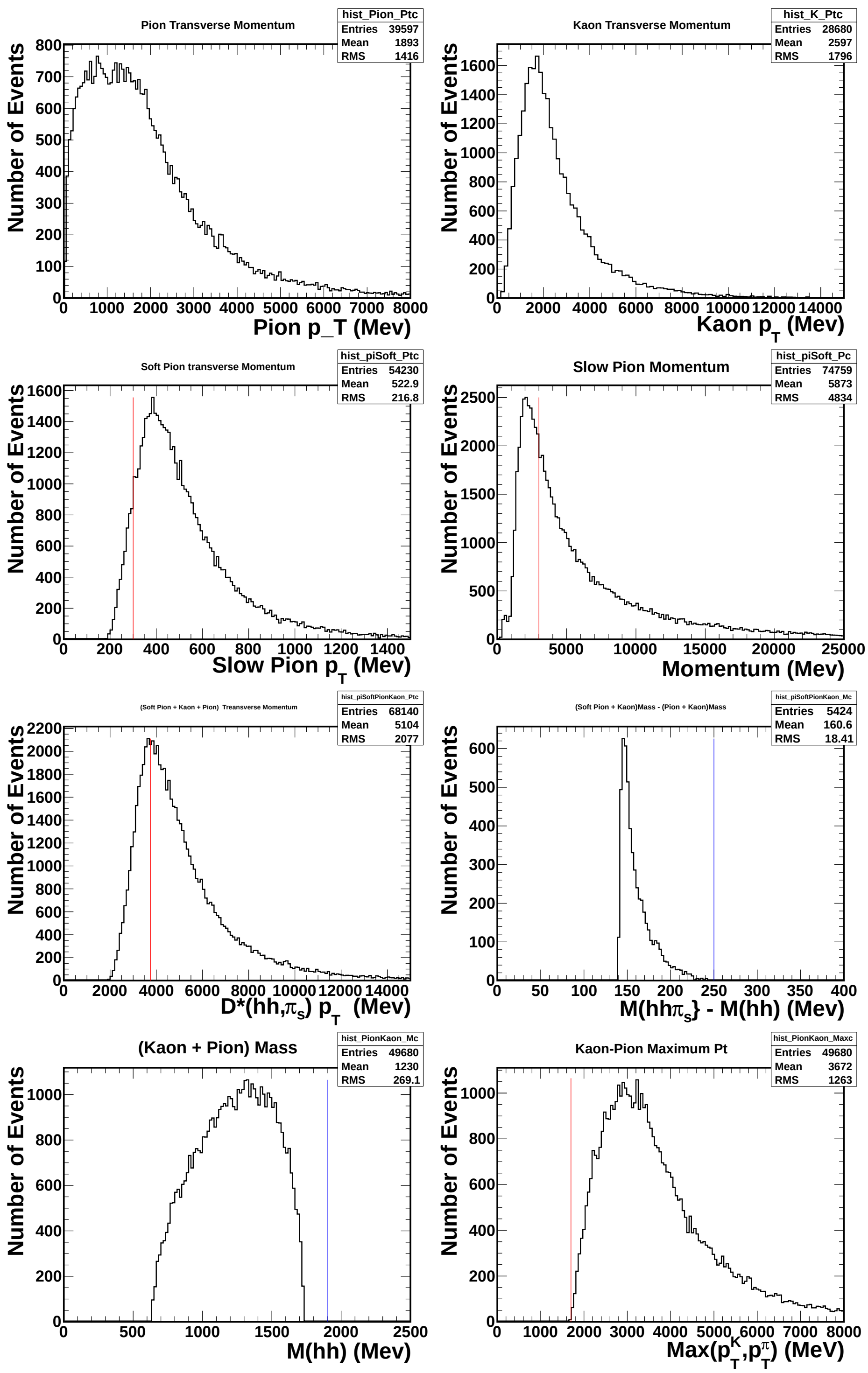

Figure 6: Selection cuts

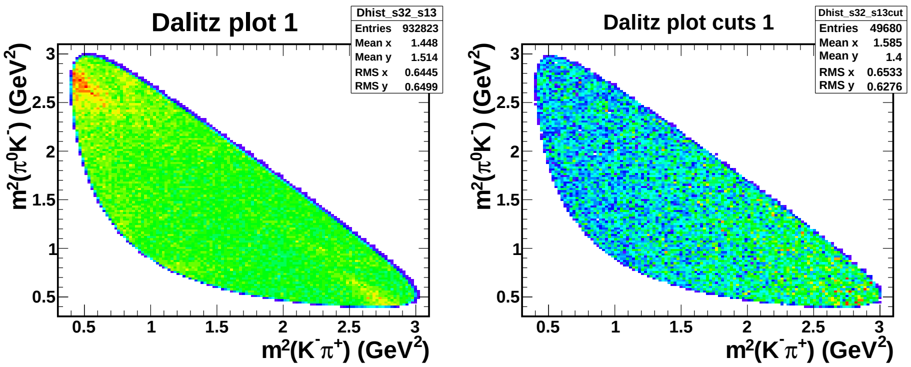

Figure 7: Dalitz plots before and after selection cuts for $D^0 \to K^-\pi^+\pi^0$

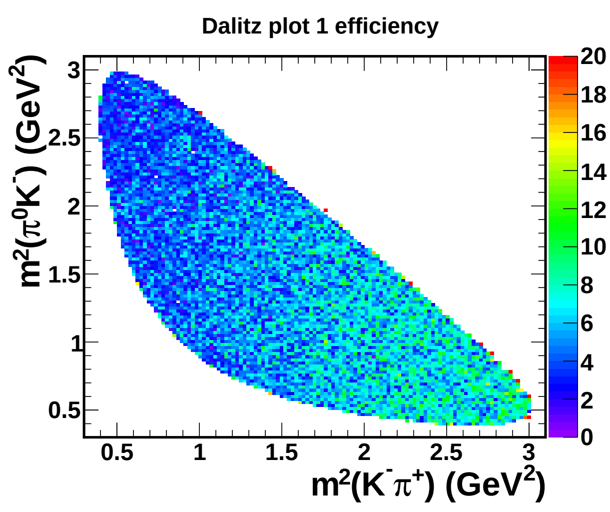

Figure 8: Efficiency across the Dalitz plot for $D^0 \to K^-\pi^+\pi^0$

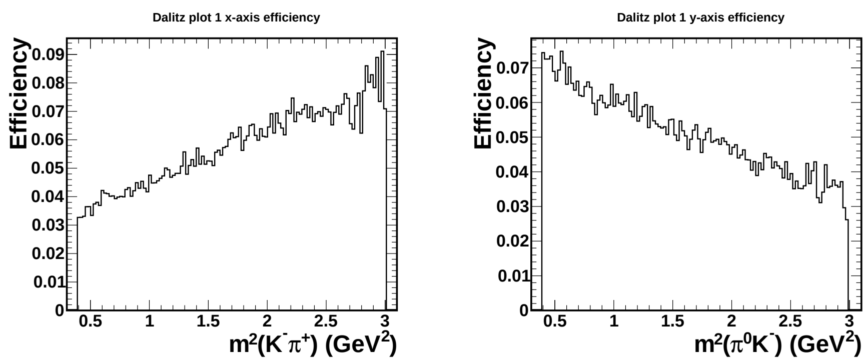

Figure 9: X-axis and Y-axis projections of the efficiency across the Dalitz plot for $D^0 \to K^-\pi^+\pi^0$

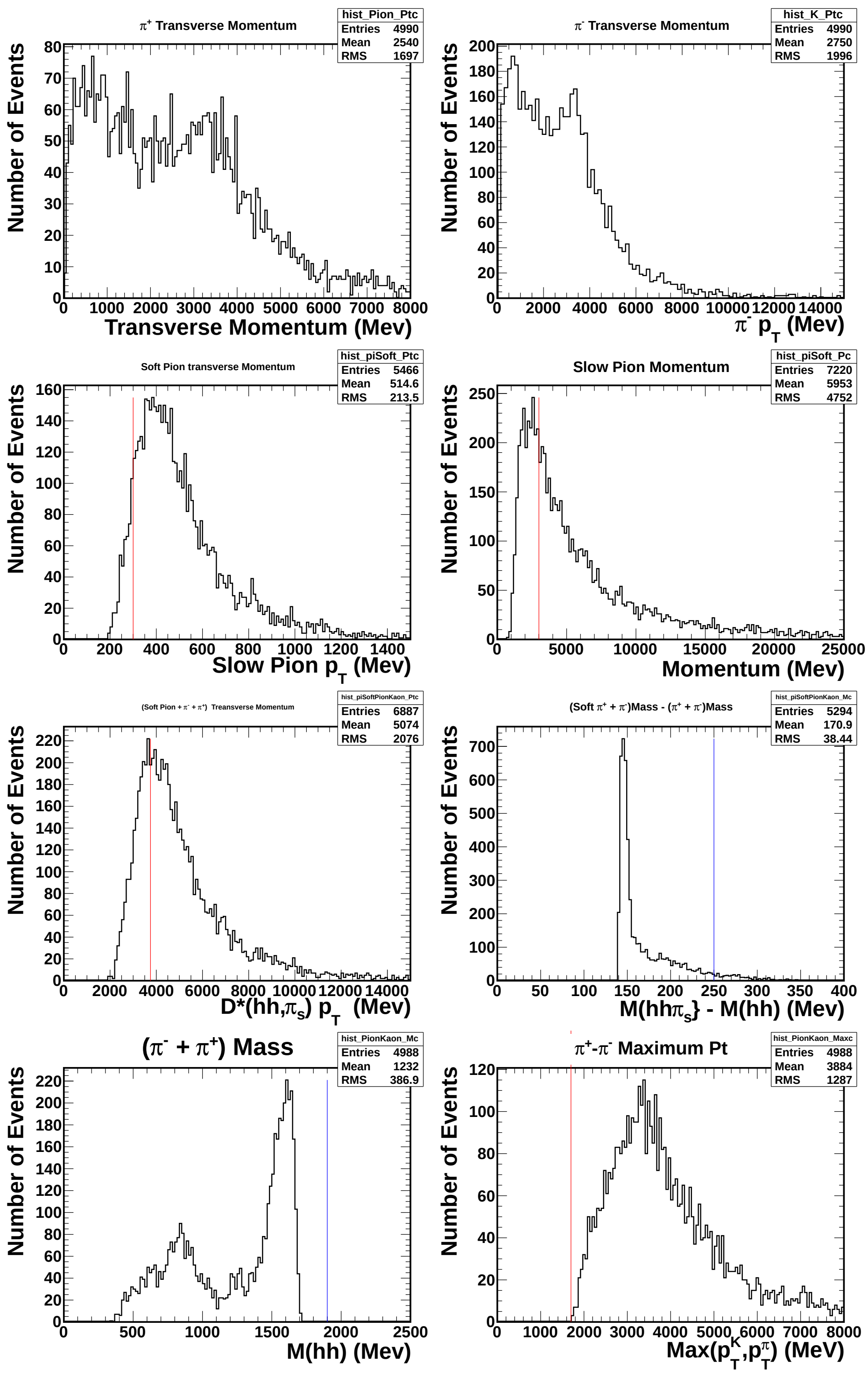

Figure 10: Selection cuts

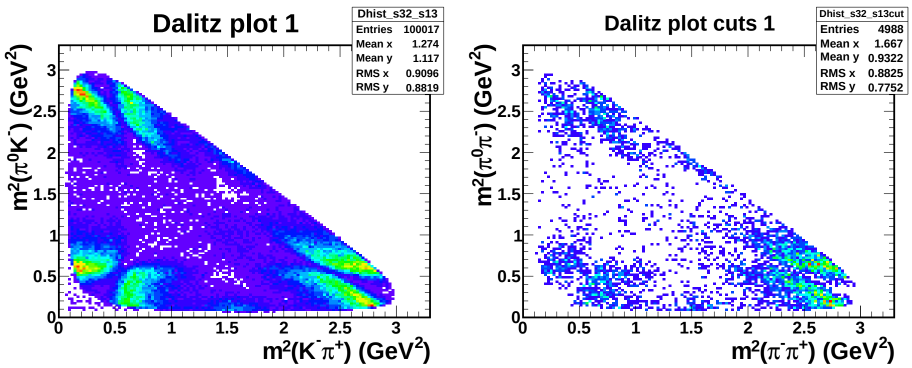

Figure 11: Dalitz plots before and after cuts for $D^0 \to \pi^-\pi^+\pi^0$

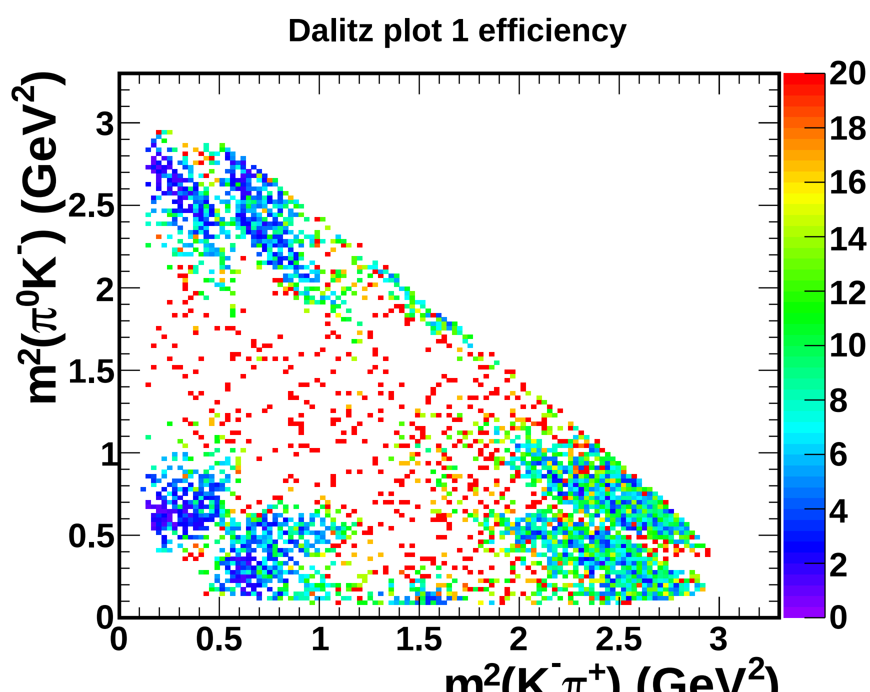

Figure 12: Efficiency across the Dalitz plot for $D^0 \to \pi^-\pi^+\pi^0$

10.5263	2.22643	0.445	0.0470648	TrkPt_SlowPion'	: 350.0 * MeV #300
				, 'TrkP_SlowPion'	: 1800.0 * MeV #3000
				, 'PT_Dstar_MIN'	: 4500.0 * MeV #3750.0 * MeV
				, 'M_MAX'	: 1900. #1900.
				, 'DeltaM_MAX'	: 200.0 * MeV #250.0 * MeV
				'PairMaxDoca_Dstar'	: 10.0 * mm
14.2105	2.53306	0.975	0.06948	TrkPt_SlowPion'	: 350.0 * MeV #300
				, 'TrkP_SlowPion'	: 2000.0 * MeV #3000
				, 'PT_Dstar_MIN'	: 3400.0 * MeV #3750.0 * MeV
				, 'M_MAX'	: 1900. #1900.
				, 'DeltaM_MAX'	: 200.0 * MeV #250.0 * MeV
				'PairMaxDoca_Dstar'	: 10.0 * mm
14.7368	2.57162	1.215	0.0774673	TrkPt_SlowPion'	: 350.0 * MeV #300
				, 'TrkP_SlowPion'	: 1500.0 * MeV #3000
				, 'PT_Dstar_MIN'	: 3000.0 * MeV #3750.0 * MeV
				, 'M_MAX'	: 1900. #1900.
				, 'DeltaM_MAX'	: 200.0 * MeV #250.0 * MeV
				'PairMaxDoca_Dstar'	: 10.0 * mm
14.7368	2.57162	1.085	0.0732539	TrkPt_SlowPion'	: 350.0 * MeV #300
				, 'TrkP_SlowPion'	: 1500.0 * MeV #3000
				, 'PT_Dstar_MIN'	: 3000.0 * MeV #3750.0 * MeV
				, 'M_MAX'	: 1900. #1900.
				, 'DeltaM_MAX'	: 210.0 * MeV #250.0 * MeV
				'PairMaxDoca_Dstar'	: 10.0 * mm
14.2105	2.53306	0.975	0.06948		
				TrkPt_SlowPion'	: 250.0 * MeV #300
				, 'TrkP_SlowPion'	: 1500.0 * MeV #3000
				, 'PT_Dstar_MIN'	: 3000.0 * MeV #3750.0 * MeV
				, 'M_MAX'	: 1900. #1900.
				, 'DeltaM_MAX'	: 200.0 * MeV #250.0 * MeV
				'PairMaxDoca_Dstar'	: 10.0 * mm
15.2632	2.60904	1.215	0.0774673	TrkPt_SlowPion'	: 235.0 * MeV #300
				, 'TrkP_SlowPion'	: 1500.0 * MeV #3000
				, 'PT_Dstar_MIN'	: 3000.0 * MeV #3750.0 * MeV
				, 'M_MAX'	: 1900. #1900.
				, 'DeltaM_MAX'	: 210.0 * MeV #250.0 * MeV
				'PairMaxDoca_Dstar'	: 10.0 * mm
14.2105	2.53306	0.975	0.06948	TrkPt_SlowPion'	: 235.0 * MeV #300
				, 'TrkP_SlowPion'	: 1500.0 * MeV #3000
				, 'PT_Dstar_MIN'	: 3000.0 * MeV #3750.0 * MeV
				, 'M_MAX'	: 1900. #1900.
				, 'DeltaM_MAX'	: 200.0 * MeV #250.0 * MeV
				'PairMaxDoca_Dstar'	: 10.0 * mm
14.2105	2.53306	0.975	0.06948	TrkPt_SlowPion'	: 235.0 * MeV #300
				, 'TrkP_SlowPion'	: 1800.0 * MeV #3000
				, 'PT_Dstar_MIN'	: 3000.0 * MeV #3750.0 * MeV
				, 'M_MAX'	: 1900. #1900.
				, 'DeltaM_MAX'	: 200.0 * MeV #250.0 * MeV
				'PairMaxDoca_Dstar'	: 10.0 * mm
14.7368	2.57162	1.215	0.0774673	TrkPt_SlowPion'	: 235.0 * MeV #300
				, 'TrkP_SlowPion'	: 1800.0 * MeV #3000
				, 'PT_Dstar_MIN'	: 3000.0 * MeV #3750.0 * MeV
				, 'M_MAX'	: 1900. #1900.
				, 'DeltaM_MAX'	: 210.0 * MeV #250.0 * MeV
				PairMaxDoca_Dstar'	: 10.0 * mm

c

10.5263	2.22643	0.445	0.0470648	TrkPt_SlowPion' : 350.0 * MeV #300 , 'TrkP_SlowPion' : 1800.0 * MeV #3000 , 'PT_Dstar_MIN' : 4500.0 * MeV #3750.0 * MeV , 'M_MAX' : 1900. #1900. , 'DeltaM_MAX' : 200.0 * MeV #250.0 * MeV 'PairMaxDoca_Dstar' : 10.0 * mm
14.2105	2.53306	0.975	0.06948	TrkPt_SlowPion' : 350.0 * MeV #300 , 'TrkP_SlowPion' : 2000.0 * MeV #3000 , 'PT_Dstar_MIN' : 3400.0 * MeV #3750.0 * MeV , 'M_MAX' : 1900. #1900. , 'DeltaM_MAX' : 200.0 * MeV #250.0 * MeV 'PairMaxDoca_Dstar' : 10.0 * mm
14.7368	2.57162	1.215	0.0774673	TrkPt_SlowPion' : 350.0 * MeV #300 , 'TrkP_SlowPion' : 1500.0 * MeV #3000 , 'PT_Dstar_MIN' : 3000.0 * MeV #3750.0 * MeV , 'M_MAX' : 1900. #1900. , 'DeltaM_MAX' : 200.0 * MeV #250.0 * MeV 'PairMaxDoca_Dstar' : 10.0 * mm
14.7368	2.57162	1.085	0.0732539	TrkPt_SlowPion' : 350.0 * MeV #300 , 'TrkP_SlowPion' : 1500.0 * MeV #3000 , 'PT_Dstar_MIN' : 3000.0 * MeV #3750.0 * MeV , 'M_MAX' : 1900. #1900. , 'DeltaM_MAX' : 210.0 * MeV #250.0 * MeV 'PairMaxDoca_Dstar' : 10.0 * mm
14.2105	2.53306	0.975	0.06948	TrkPt_SlowPion' : 250.0 * MeV #300 , 'TrkP_SlowPion' : 1500.0 * MeV #3000 , 'PT_Dstar_MIN' : 3000.0 * MeV #3750.0 * MeV , 'M_MAX' : 1900. #1900. , 'DeltaM_MAX' : 200.0 * MeV #250.0 * MeV 'PairMaxDoca_Dstar' : 10.0 * mm
15.2632	2.60904	1.215	0.0774673	TrkPt_SlowPion' : 235.0 * MeV #300 , 'TrkP_SlowPion' : 1500.0 * MeV #3000 , 'PT_Dstar_MIN' : 3000.0 * MeV #3750.0 * MeV , 'M_MAX' : 1900. #1900. , 'DeltaM_MAX' : 210.0 * MeV #250.0 * MeV 'PairMaxDoca_Dstar' : 10.0 * mm
14.2105	2.53306	0.975	0.06948	TrkPt_SlowPion' : 235.0 * MeV #300 , 'TrkP_SlowPion' : 1500.0 * MeV #3000 , 'PT_Dstar_MIN' : 3000.0 * MeV #3750.0 * MeV , 'M_MAX' : 1900. #1900. , 'DeltaM_MAX' : 200.0 * MeV #250.0 * MeV 'PairMaxDoca_Dstar' : 10.0 * mm
14.2105	2.53306	0.975	0.06948	TrkPt_SlowPion' : 235.0 * MeV #300 , 'TrkP_SlowPion' : 1800.0 * MeV #3000 , 'PT_Dstar_MIN' : 3000.0 * MeV #3750.0 * MeV , 'M_MAX' : 1900. #1900. , 'DeltaM_MAX' : 200.0 * MeV #250.0 * MeV 'PairMaxDoca_Dstar' : 10.0 * mm
14.7368	2.57162	1.215	0.0774673	TrkPt_SlowPion' : 235.0 * MeV #300 , 'TrkP_SlowPion' : 1800.0 * MeV #3000 , 'PT_Dstar_MIN' : 3000.0 * MeV #3750.0 * MeV , 'M_MAX' : 1900. #1900. , 'DeltaM_MAX' : 210.0 * MeV #250.0 * MeV PairMaxDoca_Dstar' : 10.0 * mm

Figure 13: MC and non biased trigger efficiencies